Electronic Supplementary Material (ESI) for Physical Chemistry Chemical Physics

Supplementary Material to the Paper: A Pass Too Far: Dissociation of Internal Energy Selected Paracyclophane Cations, Theory and Experiment

Patrick Hemberger,[a] Andras Bodi,[a] Christof Schon,[b] Michael Steinbauer,[b] Kathrin H. Fischer,[b] Conrad Kaiser,[c] Ingo Fischer[b]

[a] Paul Scherrer Institut, Molecular Dynamics Group, CH-5232 Villigen PSI, Switzerland
[b] Institute of Physical and Theoretical Chemistry, University of Würzburg, Am Hubland, D-97074 Würzburg
[c] Institute of Organic Chemistry, University of Würzburg, Am Hubland, D-97074 Würzburg

1 Geometries

This supplementary material lists the most important geometry parameters of the three investigated paracyclophane derivatives. In Figure S1 the numbered carbon skeleton is depicted. Bond length and angles can be found in Table S1. The twist (θ_{twist}) - and the shift (θ_{shift}) angles are calculated after the following equation:

$$\theta_{\text{twist}} = \tfrac{1}{8}\left[\theta\left(C_1\text{-}C_2\text{-}C_3\text{-}C_4\right) + \theta\left(C_1\text{-}C_2\text{-}C_3\text{-}C_8\right) + \theta\left(C_2\text{-}C_1\text{-}C_{14}\text{-}C_{13}\right) + \theta\left(C_2\text{-}C_1\text{-}C_{14}\text{-}C_{15}\right) + \theta\left(C_{10}\text{-}C_9\text{-}C_6\text{-}C_5\right) + \theta\left(C_{10}\text{-}C_9\text{-}C_6\text{-}C_7\right) + \theta\left(C_9\text{-}C_{10}\text{-}C_{11}\text{-}C_{12}\right) + \theta\left(C_9\text{-}C_{10}\text{-}C_{11}\text{-}C_{16}\right)\right]$$

$$\theta_{\text{shift}} = \tfrac{1}{8}\left[\theta\left(C_1\text{-}C_2\text{-}C_3\text{-}C_4\right) + \theta\left(C_1\text{-}C_2\text{-}C_3\text{-}C_8\right) + \theta\left(C_2\text{-}C_1\text{-}C_{14}\text{-}C_{13}\right) + \theta\left(C_2\text{-}C_1\text{-}C_{14}\text{-}C_{15}\right) - \theta\left(C_{10}\text{-}C_9\text{-}C_6\text{-}C_5\right) - \theta\left(C_{10}\text{-}C_9\text{-}C_6\text{-}C_7\right) - \theta\left(C_9\text{-}C_{10}\text{-}C_{11}\text{-}C_{12}\right) - \theta\left(C_9\text{-}C_{10}\text{-}C_{11}\text{-}C_{16}\right)\right]$$

			neutral		ion	
		exp. [1,2]	B3LYP	ωB97X-D	B3LYP	ωB97X-D
o-DHPC	R(C_1-C_2)	157	160	159	161	158
	R(C_3-C_{14})	277	281	279	277	271
	R(C_4-C_{13})	302	306	301	301	298
	R(C_8-C_{15})	308	320	316	307	303
	θ_{twist}	9	12	15	-2	11
	θ_{shift}	-6	1	0	1	9
p-DHPC	R(C_1-C_2)	159	161	159	160	158
	R(C_3-C_{14})	276	281	278	271	267
	R(C_4-C_{13})	305	312	307	303	297
	R(C_8-C_{15})	305	311	307	305	301
	θ_{twist}	0	0	0	0	-8
	θ_{shift}	13	10	15	-8	-11
MHPC	R(C_1-C_2)	158	161	159	160	158
	R(C_3-C_{14})	-	281	278	271	270
	R(C_4-C_{13})	-	311	306	306	302
	R(C_8-C_{15})	-	316	311	306	306
	θ_{twist}	-	-7	-9	-7	-14
	θ_{shift}	-	-7	-9	4	3

Table S1: Calculated geometries (in pm and °) of the neutrals and the ions. Especially in the case of *p*-DHPC a strong geometry change is observed upon ionization in the twist (θ_{twist}) and shift angle (θ_{shift}) .

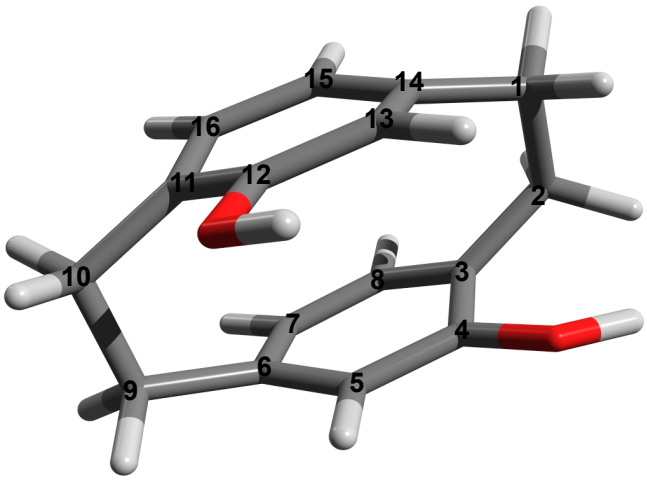

Figure S1: Numbering of the carbon atoms in the paracyclophane frame.

2 Molecular Orbitals and TD-DFT calculations

The six highest occupied molecular orbitals of MHPC are depicted in figure S2 relating to the discussion about orbitals involved in the π-π interactions in the main paper. In order to calculate more reliable vertical excitation energies TD-DFT calculations were performed (Table S2).

eV	B3LYP/6-311G(d,p)						ω-B97X-D/6-311G(d,p)					
	$\widetilde{X}$	$\widetilde{A}$	$\widetilde{B}$	$\widetilde{C}$	$\widetilde{D}$	$\widetilde{E}$	$\widetilde{X}$	$\widetilde{A}$	$\widetilde{B}$	$\widetilde{C}$	$\widetilde{D}$	$\widetilde{E}$
o-DHPC	7.38	7.61	8.03	8.69	9.82	10.45	7.57	7.70	8.37	8.91	10.29	11.04
p-DHPC	7.43	7.78	7.81	8.61	9.86	10.37	7.59[a]	7.85[a]	7.96	8.90	10.31	10.79
MHPC	7.50	7.71	8.10	8.89	9.84	10.33	7.67	7.99	8.24	9.19	10.24	10.99

Table S2: Calculated vertical transition energies to excited and ground ionic states of the three investigated paracyclophanes in eV from the neutral. $\widetilde{A}$ and $\widetilde{B}$ states are very close in energy. [a]A negative excitation value was computed and ground and excited state are therefore exchanged.

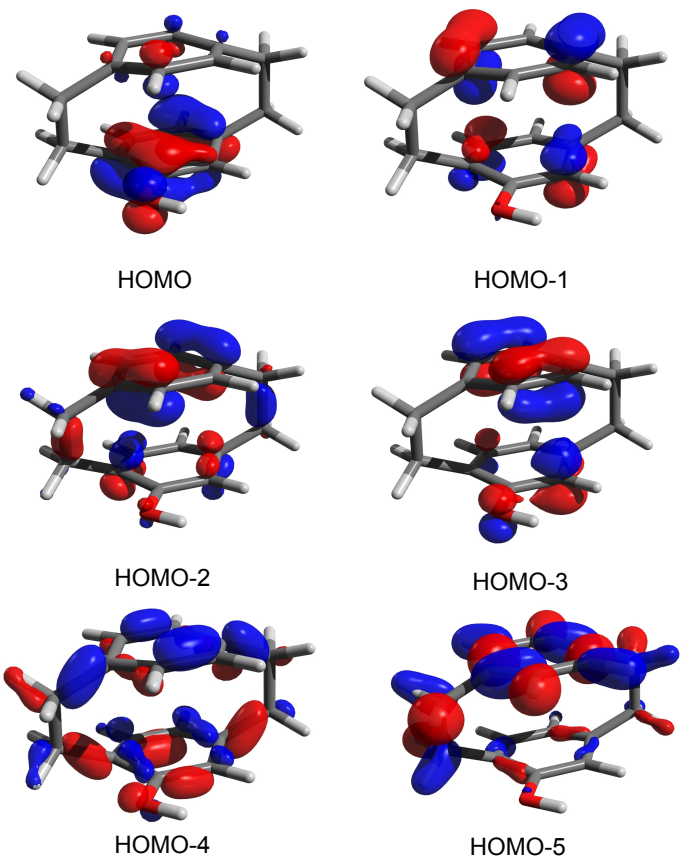

Figure S2: The six highest occupied molecular orbitals of MHPC: HOMO–2 and 3 show π-orbitals of the same phase, which makes a bonded dispersion interaction in these systems possible.

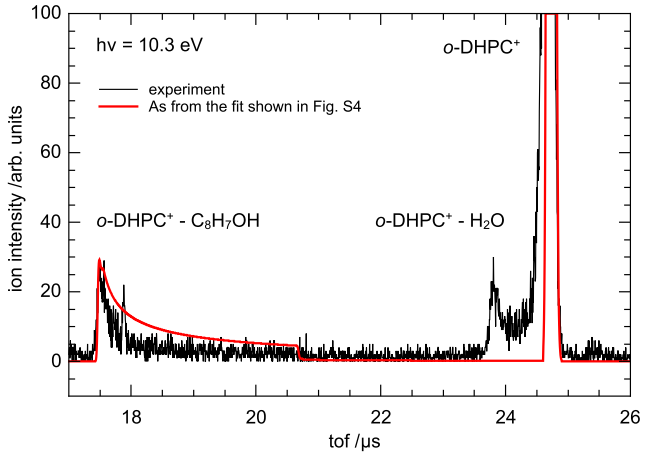

Figure S3: TOF distribution in coincidence with ***all*** electrons at 10.3 eV. Besides the main dissociation channel $C_8H_7OH^+$, also the loss of H_2O can be observed in the experiment. The red curve corresponds to the model calculation, where all vibrational modes of the ion are regarded and temperature of 470 K was assumed. Since all electrons are considered in the experimental trace, it effectively shows an integral up to 10.3 eV, and the dissociation rate constant should be much lower and the peak width, much larger than in the model, which assumes internal energy selected parents. The kinetic shift is much smaller than predicted by this model.

3 Dissociative Photoionization

Figure S3 shows a typical time-of-flight mass spectrum of *o*-DHPC in coincidence with all electrons at 10.3 eV, where apart from the $C_8H_7OH^+$ fragment also a H_2O loss channel was found. It is also clearly visible that the C_8H_7OH loss channel is only slightly asymmetric, which implies fast dissociation and only a small kinetic shift.

We also want to discuss our selected model in the light of an (ab initio statistical) model, where no ionic vibrational modes were disregarded and a sample temperature of 200 °C was assumed. Figure S4 a-c shows unreasonable fits (breakdown curve (a), CoG plot (b) and rate constants (c)) of the *o*-DHPC$^+$ dissociation. The lower temperature leads to a narrower breakdown diagram (Figure S4 a), which is not reproducing the experimental data well. If the low frequency vibrational modes of the ion were not disregarded in the model, the center of gravity plot (Figure S4 b) is shifted to higher flight times, meaning a larger kinetic shift, also indicated by slow rates (figure S4 c). This appears to be a wrong assumption, which is clarified in Figure S3, showing the calculated TOF distribution in red. Since all electrons are taken into account in this mass spectrum, the peak shape should appear broader than, if only threshold electrons were considered. In fact this in not the case so we assume that the model used in the main paper is more reliable.

In order to relate ab initio energies of the main fragmentation channel (formation of $C_8H_7OH^+$) with the experimental E_0's, we must first confirm that the latter correspond to the endothermicity of the dissociative photoionization and there is no overall reverse barrier along the reaction coordinate. In Figure S5 we show a possible reaction coordinate obtained with ω-B97X-D/6-311G(d,p) constrained geometry optimization. The first part includes the stretching of the bridge C-atoms, which passes a transition state (TS_1). During the dihedral scan of the intact CH_2–CH_2 bridge another minimum was found (2). Further enlargement of this angle yields a transition state (TS_2), which corresponds to the rotational barrier of the OH group, and leads to an open s-shaped structure (3). At this point the remaining bridge between the two rings was stretched, giving two

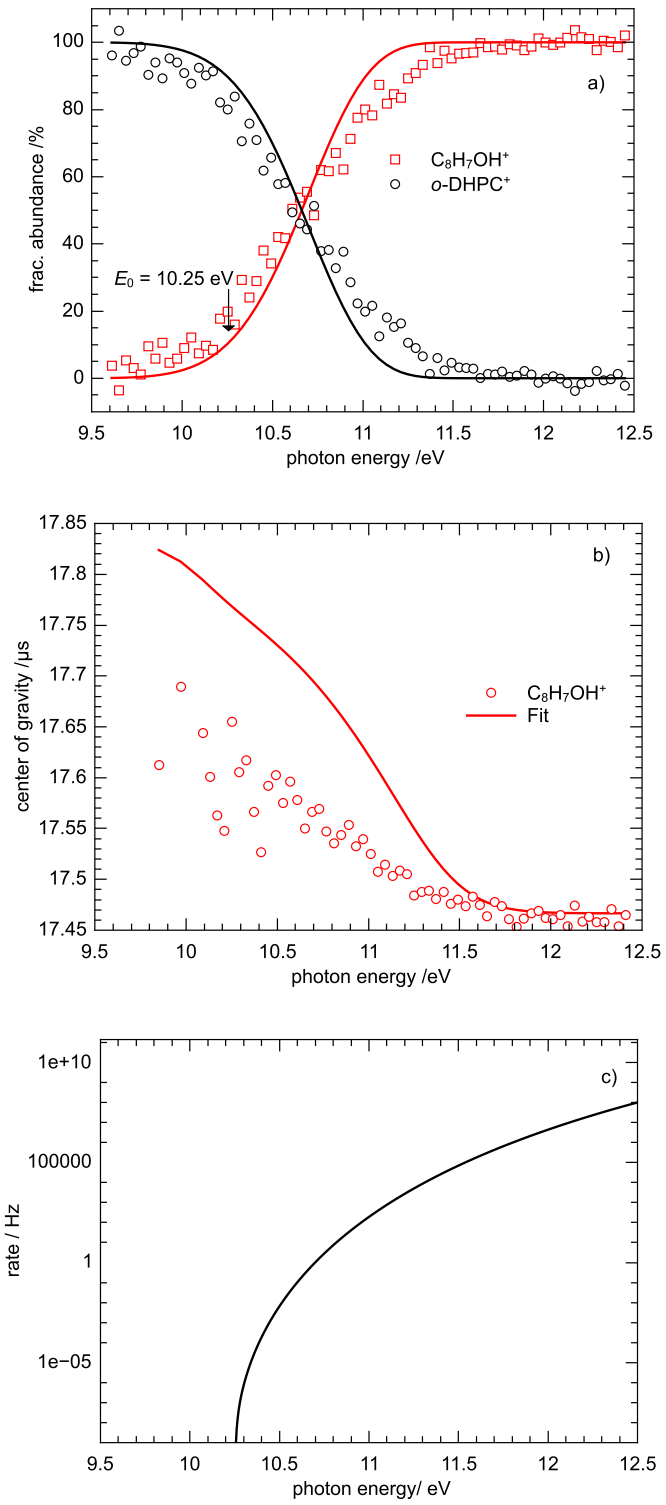

Figure S4: (a) fitted breakdown diagram of *o*-DHPC with a more realistic temperature of 470 K. (b) center of gravity plot the rates are not well described by the model. The overestimated kinetic shift moves the E_0 to 10.25 eV.

hydroxy-xylylenes (4). Structures 1–4 in figure S5 are real minima without any imaginary frequencies. Both transition states TS_1 and TS_2 were obtained in a constrained geometry scan with a subsequently performed vibrational frequency calculation. In the absence of an overall reverse barrier the experimental appearance energy corresponds to the dissociative photoionization energy.

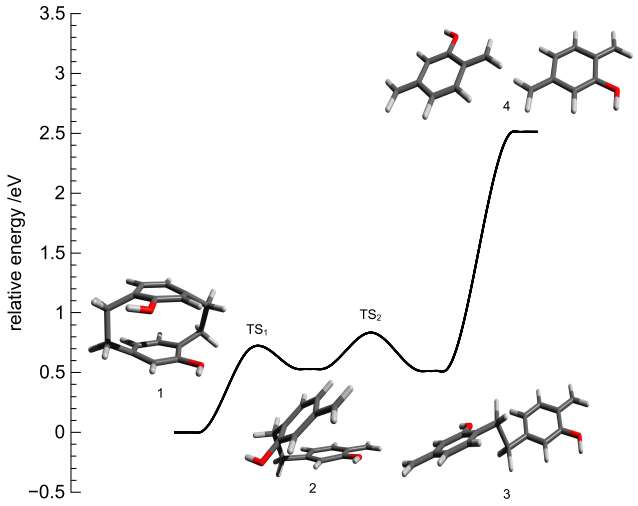

Figure S5: Reaction coordinate of the dissociation of *o*-DHPC. Three different constrained geometry scans were performed. Those are the elongation of the CH_2–CH_2 bridge carbon atoms, giving transition state TS_1 and during the dihedral scan a minimum structure 2 was obtained. Further scanning of this coordinate another TS_2 was obtained, which corresponds to the rotational barrier of the OH group. The s-shaped structure 3 is also a minimum. Finally the remaining CH_2–CH_2 bridge was elongated and two hydroxy-xylylenes (4) were generated.

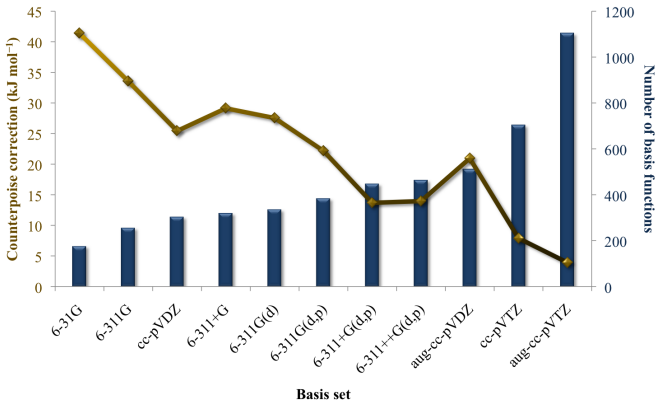

Figure S6: Counterpoise correction in paracyclophane (left scale) as a function of basis set and its size (right scale), with respect to the xylylene fragments obtained with the M06-2X functional. The correction drops to below 15 kJ mol^{-1} with the 6-311+G(d,p) basis set, and below 5 kJ mol^{-1} with the aug-cc-pVTZ basis set. It was performed by methods known to the literature.[3] In brief, two xylylene fragments were calculated in their distored structure as they can be found in the parent paracylophane.

References

[1] J. Pfister, C. Schon, W. Roth, C. Kaiser, C. Lambert, K. Gruss, H. Braunschweig, I. Fischer, R. F. Fink and B. Engels, *J. Phys. Chem. A,*, 2011, **115**, 3583–3591.

[2] B. Kovac, M. Mohraz, E. Heilbronner, V. Boekelheide and H. Hopf, *J. Am. Chem. Soc.*, 1980, **102**, 4314–4324.

[3] P. Valiron and I. Mayer, *Chem. Phys. Lett.*, 1997, **275**, 46–55.